Hundred-Picoseconds Electro-Optical Switching With Semiconductor Optical Amplifiers Using Multi-Impulse Step Injection Current

Rafael C. Figueiredo, Napoleão S. Ribeiro, Antonio Marcelo Oliveira Ribeiro, Cristiano M. Gallep, *Member, IEEE*, and Evandro Conforti, *Life Senior Member, IEEE*

***Abstract*—An ultrafast electro-optical amplified switch based on chip-on-carrier semiconductor optical amplifier with high optical contrast (33 dB) is presented. Switching times up to 115 ps with small overshoot were achieved by using the multi-impulse step injected current technique. These results are compared with previous preimpulse step injected current technique, and achieve a reduction of the inherent, post switching gain fluctuations without worsening the switching times. In addition, pulse formats for controlling such a kind of electro-optical switches are numerically analyzed and compared with experiments.**

***Index Terms*—Electro-optics switches, optical switches, semiconductor optical amplifiers.**

I. Introduction

MODERN data centers are at fast growing pace due to the exponential increase of network traffic as a consequence of speedy raising number of web services and applications [1]. Data center network (DCN) servers can be interconnected according to a fault tolerant flat tree topology network, where the servers are connected through a Top-of-the-Rack Switch (ToR) and these ToRs are further interconnected by clusters and aggregate switches [2]. The switching is there performed by electronic packet switches, at each level of the tree topology. In such topology, the flattening of the inter-cluster DCN can be implemented by photonics technologies, enabling optically transparent switching and interconnection, avoiding so the costly, high speed OEO (optical-electrical-optical) conversions and the electronic buffers.

One problem to be solved is the ToR switching latency between the nodes. The latency impacts the completion time in some applications.

Manuscript received July 22, 2014; revised October 10, 2014 and November 15, 2014; accepted November 16, 2014. Date of publication November 19, 2014; date of current version December 16, 2014. This work was supported in part by Fotonicom-INCT-CNPq and Fapesp (Padtec, # 2007/56024-4), Brazil.

R. C. Figueiredo, N. S. Ribeiro, A. M. O. Ribeiro, and E. Conforti are with the Department of Communications, Faculty of Electrical and Computer Engineering, University of Campinas, Campinas, SP 13083-970, Brazil(e-mail: rafael.figueiredo@gmail.com; napoleaoribeiro@gmail.com; aribeiro@dmo.fee.unicamp.br; conforti@ ieee.org).

C. M. Gallep is with the Department of Communications, Faculty of Electrical and Computer Engineering, University of Campinas, Campinas, SP 13083-970, Brazil, and also with the Division of Telecommunication Technology—School of Technology, University of Campinas, Limeira, SP 13484-370, Brazil (e-mail: gallep@ft.unicamp.br).

Color versions of one or more of the figures in this paper are available online at http://ieeexplore.ieee.org.

Digital Object Identifier 10.1109/JLT.2014.2372893

The semiconductor optical amplifier (SOA) can be a useful device to reduce this latency, since an N × N SOA switch can establish connections between ports in nanoseconds [3], [4]. Recently, an optical flat DCN based on scalable optical switch system with optical flow control, employing SOAs in 1 × N switches, achieved an average latency less than 500 ns and an overall power consumption of 37.25 pJ/bit [5]. In addition, the amplification introduced by the SOA switch was used to compensate the splitting losses of the broadcast stage [6].

The overall DCN latency depends of many factors, such as link length, the control architecture, the packet guard times, and the optical flow control. However, the reduction of the SOA electro-optical (EO) switching time could further reduce the DCN latency [7]. The reduction of transit times in EO switches based on pre-distorted control signals was tested first for boosting the speed of laser-based switches [8]. Regarding the SOA—basically a laser with non-reflective edges—similar predistortion technique was first called "Pre-Impulse Step Injected Current," (PISIC) [7]. Such technique was later improved to achieve optical contrast above 25 dB, with *off-on* SOA switching time reduction from 2000 to 650 ps [9]. Spurious output power fluctuations that are inherent to the process, and its minimization within compromise with improved switching times were analyzed further in [10]. In addition, this technique could also be applied to improve direct modulation of vertical-cavity surface-emitting lasers (VCSEL), which are widely used in optical interconnects [11].

By using numerical analysis based on equivalent circuits (ECs) it was confirmed that the packaging electrical parasites—inductances and, mainly, capacitances—are the restriction for further improvement of switching speeds and also reduction of output power fluctuations. Moreover, an EC whose results agree with the experimental data was obtained, enabling simulation of new switching pulses formats [12].

Reduction of electrical parasitic is achieved here using a microstrip directly coupled to a chip-on-carrier (COC) SOA, excluding so the standard butterfly encapsulation. In addition, a new technique employing multi-impulse step injected current (MISIC) is presented to reduce the output power overshoots [10] and so avoid deterioration in switching windows. Experimental results obtained for a SOA-based EO switch using the PISIC and the MISIC formats are shown, with analysis of the switching time improvement and the overshoot minimization. Switching times below 115 ps were achieved with optical contrast up to 29 dB and overall optical overshoot reduction of

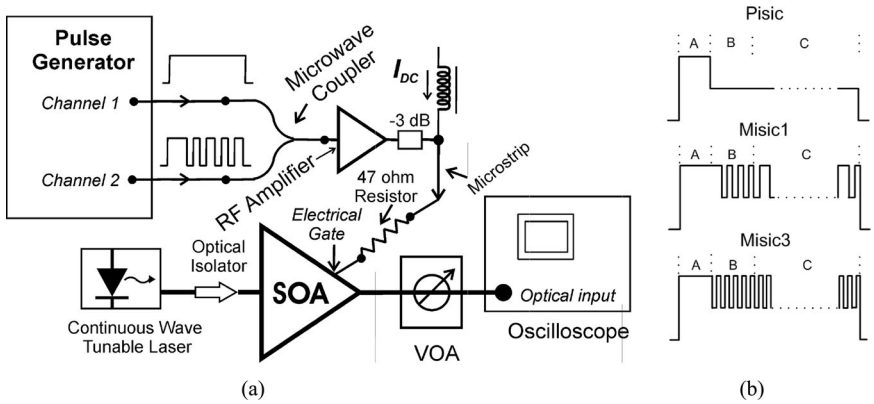

Fig. 1. (a) Experimental setup for electro-optical switching analysis, (b) example of PISIC and MISIC formats.

50%. In addition, numerical results from the EC modeling are compared to experimental data.

II. Experimental Setup

The experimental setup is shown in Fig. 1. The optical setup contains a CW tunable semiconductor laser, an optical isolator, a commercial SOA-COC, a variable optical attenuator, and a 40 GHz digital communication analyzer with optical input port. The SOA-COC is the COC version of NL-OEC-1550-CocMW651 (CIP, U.K.), a MQW device with 2-mm-long active cavity, absolute maximum drive current of 400 mA, 1550 nm saturation output power of 9 dBm, and small signal gain of 31 dB at 200 mA, with fiber coupling loss of 1.8 dB, noise figure of 9 dB. The use of a SOA-COC demand suitable temperature control system, two five axis positioners with piezoelectric controllers to move fibers with microlens, and so couple light into/out of the device with an optical insertion loss of 9 dB each.

In the electrical setup the pulse generator is a fundamental module, enabling different composite pulse formats that are further combined to switch the SOA. The generator (Agilent J-BERT N4903B) has two separate outputs channels for two independent pulse formatting: each one is constructed by different bit sequences (bit window = 80 ps). The two electrical outputs channels are combined (50 GHz bandwidth resistive combiner) and amplified. The resultant electrical pulses are injected into the SOA-COC using a 50 Ω low inductance series resistor, providing the impedance matching ($Z_{SOA} \sim 3.5\ \Omega$), after addition of bias current (I_{DC}, by a 40 GHz bandwidth bias-T). The microwave amplifier setup shown comprises a tap to visualize the electrical signal, amplifiers and matching circuits. A 3 dB attenuator was included between the amplifier output and the SOA gate to reduce back-and-forth reflections, and to protect the amplifier against variations of SOA impedance. The components have a minimum bandwidth of 35 GHz. The maximum applied signal to the SOA electrical gate is limited to 6.4 Vpp. Therefore the maximum current excursion is 120 mA—so, considering I-bias of 80 mA, the injected current will have an excursion from 20 to 140 mA. However, if the pre-impulse is also considered with the step, the current excursion will change from 120 mA to 90 mA (step—4.7 V and impulse—1.7 V) or 50 mA (step—2.7 V and impulse—3.7 V).

Typical PISIC and MISIC formats are illustrated at Fig. 1(b). Basically, three sectors are conformed to optimize the EO switching: the pre-impulse part "A," the immediate sequence part "B" and the final part "C." PISIC format is shown in the superior trace of Fig. 1(b): it has just an impulse in the "A" section plus the normal step signal. The Misic1 and Misic3 are shown in the medium and inferior traces of Fig. 1(b). MISIC formats have an impulse in the part "A" but also have impulses in parts "B" and "C." Proper impulses durations and amplitudes used in part "B" may minimize the initial output overshoot; part "C" may counteract the relaxation oscillations during the switching window by injecting short current pulses, as shown next.

The switch step response is shown in Fig. 2. Fig. 2(a) illustrates a typical electrical 8 ns step pulse, using just one generator channel at maximum voltage (6.4 V), after RF amplification. The pulse rise time is 50 ps in this case. The CW laser provides maximum optical power of 5 dBm, leading to SOA Pin = −4 dBm, giving the best switching times. Tests for smaller Pin were performed as well (not shown), with response speed decreased depending on format of composite pulse. For SOA Pin = −14 dBm, for example, switching time increases in 10% to 20% depending on pulse format.

The SOA net optical gain *versus* current characteristic is shown at Fig. 2(b). The Fig. 2(c) shows the output optical signal (considering insertion losses) in response to the drive signal of Fig. 2(a), when maximum optical contrast is achieved (33 dB).

III. Experimental Results

The switching performance obtained for different pulse formats are presented in this section, starting by the most simple format—single step—whose results are compared to the ones obtained by composite pulses, always aiming to reduce switching times and fluctuations in the output power.

A. Step

The simplest version for the current injection format is a fast-rise step signal, as shown at Fig. 2(a). The step duration is 8 ns (100 bits), followed by another 8 ns at the lower level,

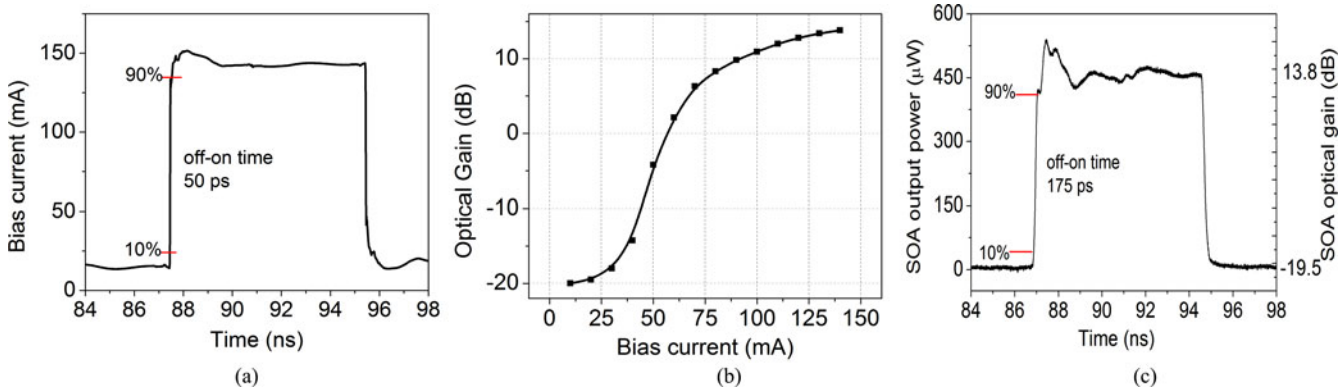

Fig. 2. (a) Electrical step, $I_{\mathrm{DC}} = 80$ mA, (b) optical gain curve of the SOA-COC, (c) SOA-COC optical response for electrical input of (a).

giving so enough time for the active cavity to be filled up, by the injected current and to stabilize in steady-state condition. This time window is used for all results presented here.

The optical response to that, as in Fig. 2(c), presents an *off-on* rise time (10–90%) of 175 ps, an improvement of 3.7 times in relation to the results presented in previous works (650 ps) [9], [10]. This improvement can be associated to the use of SOA-COC with a higher bandwidth (≈40 GHz) microwave setup, and to the higher optical gain due the longer SOA (2 mm) used here; while the previous results were achieved for encapsulated, 0.65-mm long SOAs [9], [10].

Despite the small switching time, the optical response shows power overshoot (16%) and spurious fluctuations following that. This overshoot arises in response to the huge current step and it is an intrinsic SOA response. For a step from 45 to 115 mA, a similar *off-on* time was noted (170 ps) but with higher overshoot (18%) and smaller optical contrast (21.5 dB).

B. Pre-Impulse Step Injected Current

There is a minimum time for the SOA to turn on since the active region, initially empty, must be populated by the injected current, and so the optical gain changes. The SOA's optical gain increases with a time constant comparable to that of electrical carrier lifetime, at the beginning of the current step rises. The so-called carrier lifetime is not really a constant value since it changes with the population density, both electrical and optical [11]–[13]. A high but short current pulse can be so used to quickly increase the carrier population, decreasing so the SOA carrier lifetime and enabling reduction in switching times. In this sense, the PISIC technique is demonstrated to decrease the *off-on* times.

Fig. 3(a) shows the electrical pulse constructed with PISIC – a pre-impulse combined with the step. To do that, the two generator outputs are combined before the RF amplification. The electrical rise time (50 ps) is the same as before. However, the optical output power contrast is reduced to 29 dB (due the RF amplifier saturation), but the *off-on* rise time has almost 35% reduction, to 115 ps (see Fig. 3(b)).

The pre-impulse has some features that can be modified in order to contribute to decrease the *off-on* times. The analysis of the pre-impulse width and amplitude were made (not shown here). The best result is shown here, for a composite pulse of 6-bit width (0.48 ns) and maximum amplitude. The width and amplitude choices were made by considering the better relation for *off-on* time *versus* overshoot, considering the limit of 30% for the overshoot.

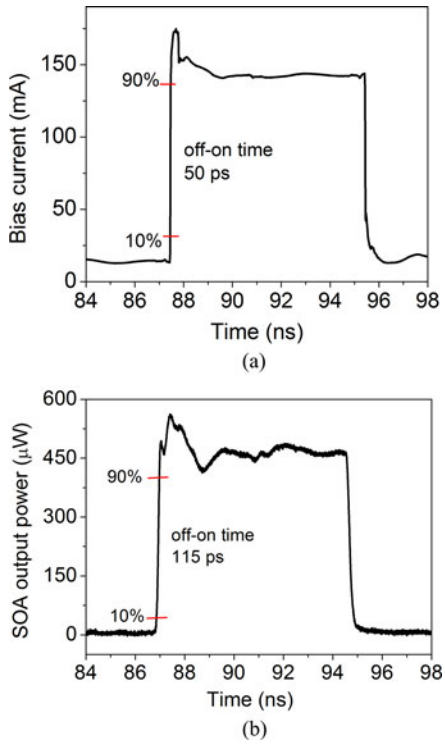

Fig. 3. (a) PISIC format ($I_{\mathrm{DC}} = 80$ mA), (b) SOA optical response to (a).

On the other hand, the PISIC overshoot increases to 25% due to the additional current injected with the pre-impulse. Fig. 4(a) and (b) illustrate this comparison of a single-step to the PISIC technique—the rising time reduction is detailed in the inset zoom. Fig. 5(a) shows the optical response for a simple step current and for PISIC format with step amplitude of 2.7 V and pre-impulse of 3.7 V. The overshoot increases to 63% with the PISIC technique. The overshoot value is excessive if compared with the established limit (30%), although the off-on time decreased. Therefore, it would be interesting to have a technique

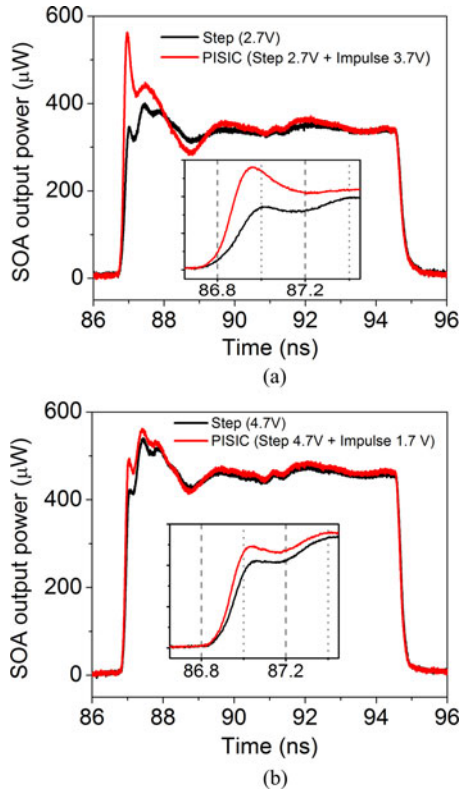

Fig. 4. Optical response for single step and PISIC bias current formats ($I_{\mathrm{DC}} = 80$ mA), with impulse = 3.7 V and step of 2.7 V (a) and impulse = 1.7 V and step of 4.7 V(b).

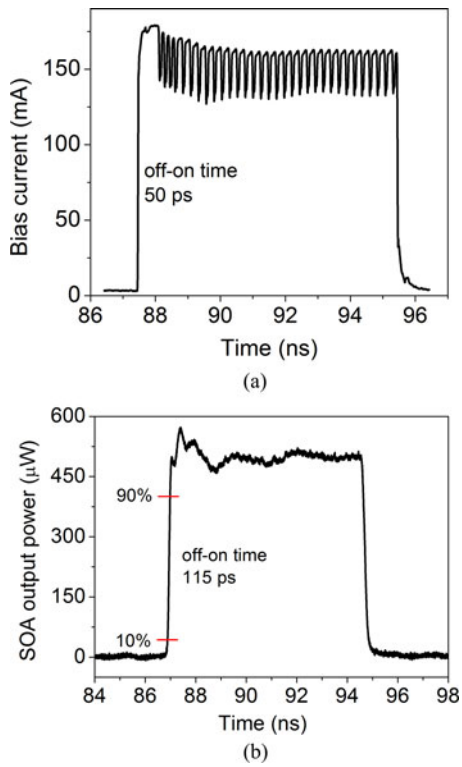

Fig. 5. (a) Misic1 electrical pulse ($I_{\mathrm{DC}} = 80$ mA) (b) SOA optical response to (a).

TABLE I
MISIC FORMATS

	Multi-impulses (100 bits)		
	Sections		
	A	B	C
Misic1	111111	11010101	011 011 011 011
Misic2	111111	01101101	1 011 011 011 110
Misic3	111111	01010101	0101 0101 0101
Misic4	010101	01010110	1 011 011 011 011
Misic5	011011	01010110	11 011 011 011
Misic6	111111	11111111	1111 1111 1111

that could reduce the overshoot without increasing the off-on times, since high overshoots may disturb decision level to be chosen at the receiver at the end of the optical link. Fig. 5(b) illustrates this comparison between a simple step injected current and the PISIC with step amplitude of 2.7 V and pre-impulse of 3.7 V. In this case the SOA-COC gain is saturated due to high injected current and thus the overshoot is not too high.

C. Multi-Impulse Step Injected Current

By observing the optical response obtained by the PISIC format it is possible to analyze the effect of a proper sequence of pulses (i.e., bits in the signal generator) to reduce the initial overshoot and the fluctuations without increasing the *off-on* time. This was done by combining different bit sequences from the two independent electrical channels, as presented in Table I.

Fig. 5(a) illustrates one kind of MISIC (Misic1) built with a step followed by multiples impulses (see Table I), in a total of 100 bits. Fig. 5(b) shows the correspondent SOA optical output. The impulse sequence contributes to increase the bias current average level. However, due to the upper level (140 mA) being near to the gain saturation, higher bias currents modify a little the optical contrast from 29 dB (Step and PISIC) to 30 dB (Misic1). The optical response shows a slightly increase of the upper level (but not sufficient to modify the *off-on* time) and overshoot reduced to 12.5%. The price to pay is the higher power consumption, since the energy to switch the SOA increases from 9.1 nJ (Step and PISIC) to 10.4 nJ (Misic1), i.e., an increase of 15%. Those energy levels were estimated from the electrical power calculated using 8-ns-long, composed pulses used to switch the SOA (see Figs. 4(a) and 5(a)). However, the MISIC impulses also increase the SOA gain.

Table II presents the optical contrasts obtained for all cases, with good performance (>25 dB), with steps of 4.7 V. The estimated error is less than 1 dB due to optical mount instabilities to obtain Fig. 2(b), and considering the optical signal after the SOA gain was stabilized. Fig. 6 illustrates the *off-on* switching times and correspondent overshoot values (%) obtained for the MISIC formats. In both cases—2.7 and 4.7 V for the step signal—the Misic1 format has better results, reducing the overshoot and *off-on* times. Steps with 2.7 V promote lower bias currents, below the gain saturation levels and so contribute to enhance the technique efficiency.

TABLE II
OPTICAL CONTRAST

Pulse	I_{DC} = 60 mA		I_{DC} = 80 mA	
	Step 2.7 V Impulse 3.7 V	Step 4.7 V Impulse 1.7 V	Step 2.7 V Impulse 3.7 V	Step 4.7 V Impulse 1.7 V
Step (6.6 V)	29 dB	27 dB	27 dB	32 dB
Pisic	25 dB	31.5 dB	12.5 dB	29 dB
Misic1	27 dB	32 dB	17 dB	30 dB
Misic2	27 dB	32 dB	17 dB	30 dB
Misic3	27 dB	32 dB	17 dB	30 dB
Misic4	27 dB	32 dB	17 dB	30 dB
Misic5	27 dB	32 dB	17 dB	30 dB
Misic6	28.6 dB	33 dB	18 dB	32 dB

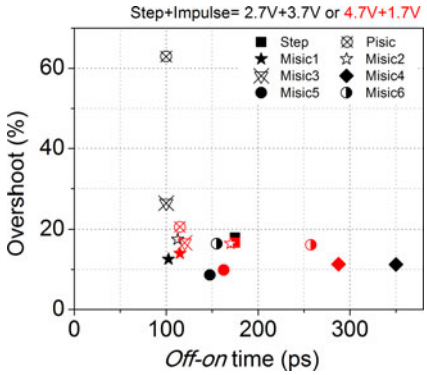

Fig. 6. Overshoots and *off-on* times for different pulse formats (I_{DC} = 80 mA, preimpulse of 3.7 V and step of 2.7 V or preimpulse of 1.7 V and step of 4.7 V).

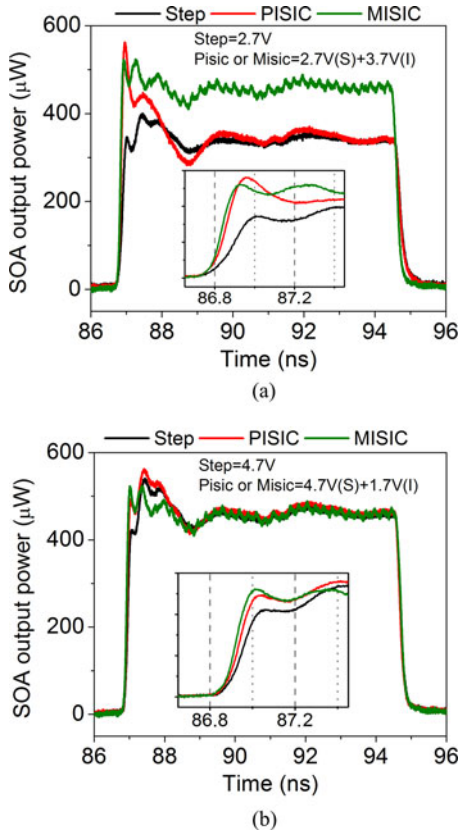

Fig. 7. Optical responses for a single step bias current, PISIC, and Misic1 formats (I_{DC} = 80 mA), with impulse = 3.7 V and step of 2.7 V (a) and impulse = 1.7 V and step of 4.7 V (b).

The Misic4 format presented the worst result. Although it reduces the overshoot there is a large increase in the *off-on* time. Misic2, Misic5, and Misic6 reduce the overshoot but increase the switching times. The optical responses for the simple step, the PISIC and Misic1 formats are shown at Fig. 7, for impulse of 3.7 V and step of 2.7 V (a) and impulse of 1.7 V and step of 4.7 V (b).

The advantage of MISIC is clearly seen in relation to PISIC (reduction of overshoot), and in relation to step (reduction of rise time). The upper level of MISIC presents small fluctuations and this might be a consequence of the interaction between MISIC impulses and SOA carriers relaxation, since the impulses of MISIC1 shown in Fig. 5(a) repeat every 240 ps (4.16 Gb/s) with first harmonic around 2 GHz that is close to the SOA relaxation oscillation frequency. In addition, the SOA response also presents undershoot that is more pronounced just after the rise time. In those cases MISIC has advantage over PISIC as shown in Fig. 7(a), for example.

IV. SIMULATION RESULTS AND DISCUSSION

The COC SOA microwave mount is shown at Fig. 8 (not to scale), where the 2.4 mm connector after the microwave amplifier (see also Fig. 1) should be soldered at the beginning of a 32-mm-long microstrip line. The microstrip edge is soldered

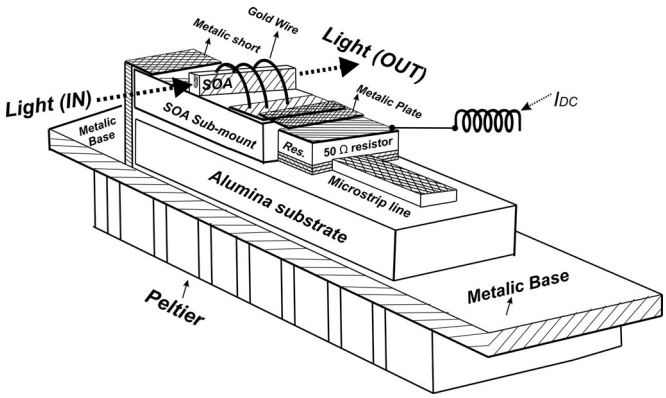

Fig. 8. SOA microwave mount and its components.

to a low inductance 50 Ω resistor. The other resistor termination is pressed over the SOA sub-mount by a metallic gold plate, in such a way that the sub-mount could be exchanged. The miniature choke is also soldered on this resistor terminal to allow bias current injection. The SOA sub-mount is made with a intrinsic silicon block, 10 mm × 2 mm × 1 mm. The metallic plate is also connected to the SOA chip using three 2-mm-long gold wires. The other SOA's electric termination is soldered over a gold metal film, and this film is attached to a solid metal, grounded. Two five-axis fiber positioners with piezo controllers

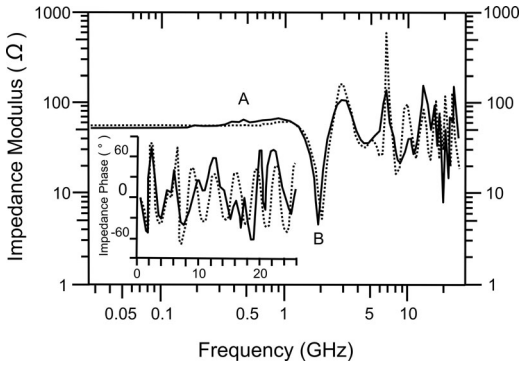

Fig. 9. Experimental (solid line) and theoretical (dotted line) SOA microwave mount input electrical impedance modulus and phase.

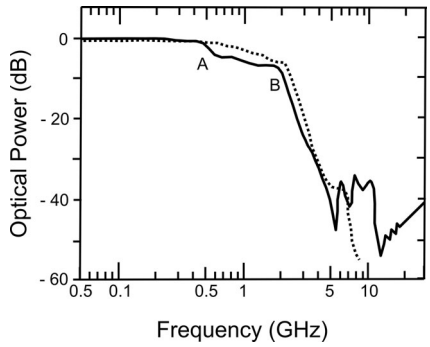

Fig. 10. Experimental (solid line) and theoretical (dotted line) SOA optical output normalized power versus the microwave injected current frequency (SOA bias of 60 mA and −10 dBm optical input power).

provide the collimated light to/from the SOA, with an estimated 9 dB optical insertion loss each side. The alumina substrate of the microstrip line is placed over a metallic base, and everything is attached to a Peltier element for temperature control. In this way, the Peltier is isolated from the microwave signal, avoiding extra parasitics.

A SOA small-signal, ac electrical EC was used for simulations [14], [15]. The EC of the microwave mount itself (see Fig. 8) is obtained using the reflected microwave signal at the plane of the microstrip line edge (impedance modulus and phase), shown at Fig. 9. A movable, miniature short-circuit gate was used here to take out the SOA effect, and this procedure is enough to obtain the electrical fixed parameters, without the SOA. However, to find the EC for chip SOA it is also necessary to measure the output optical power when a small amplitude microwave current is injected, for a fixed optical input power (−10 dBm and 60 mA), as shown at Fig. 10. The frequency domain analysis can be initiated using the EC for a laser [15]. By using ADS software (Keysight Techn.) and all measured data the circuit can be progressively adapted until the final design is reached heuristically, as shown at Fig. 11. This EC is a small-signal model, and it is preserved when the bias is varied. However, the values of some of its elements change with I-bias and optical input power.

Reasonable agreement between theoretical and measured values was obtained using the EC of Fig. 11, up to 26 GHz, as shown

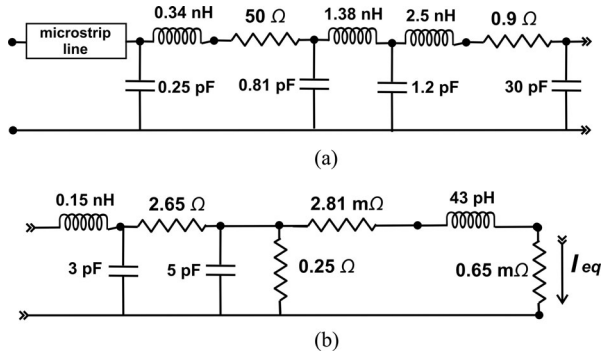

Fig. 11. Equivalent circuit for the SOA mount of Fig 8 (at 60 mA SOA bias). (a) The upper part represents the microwave injection current has fixed values and should be directly connected to the (b) lower part representing the SOA.

at Figs. 9 and 10. Also it is noted that the SOA normalized output power decreases when the injected current reaches 0.5 GHz (point A of Fig. 10), going deeply down after 2 GHz (point B). Also the impedance modulus goes to 5 Ω at 2 GHz. This B frequency is related to the SOA relaxation oscillations and has an important rule for electro-optical switching. It is also important to note that the EC has a front part, shown at Fig. 11(a), whose parameters are fixed, and another part in series, at Fig. 11(b), where the circuit parameters do change with the I-bias and optical input power. Approximately the elements of Fig. 11(a) can be related as follows: the 0.25 pF and the 0.34 nH are the 50 Ω resistor parasitics; the 0.81 pF and the 1.38 nH are the metallic plate parasitics; the 1.2 pF, 2.5 nH, the 0.9 pF, and the 30 pF are the parasitic of the plate and wires of the SOA sub-mount. The elements of Fig. 11(b) can be related as: the 0.15 nH, the 3 pF, and the 2.65 Ω resistor are SOA chip intrinsic parasitics; the 5 pF is the space charge plus the diffusion SOA capacitances [15]; the 0.25 Ω the "diffusion resistance," the stray inductance of 43 pH, the stray resistances of 2.81 and 0.65 mΩ represent the SOA active region [15]; and the current I_{eq} passing this last resistor is proportional to the SOA optical output power.

The results employing the EC of Fig. 11 are shown in Fig. 12(a) and (b), for the PISIC and the MISIC, with step of 4.7 V and impulse of 1.7 V with bias of 60 mA. Both results predict a slower rise time of 170 ps in relation to the experiment (115 ps). Considering that this step would provide a current excursion of 60 mA $\pm$ 4 mA, the SOA would be below transparency to gain saturation during the *off-on* excursion (see Fig. 2(b)). However, during the impulse window a very high number of carriers would be generated since in a very short time the SOA go in to deeper saturation (peak current of $60 + 44 + 32$ mA). The EC model based on small signal analysis [15] cannot predict nonlinear behaviour provoked by large signal as those, and the theoretical results are a first approximation. In addition, the simulated results predict signal fluctuations with higher amplitude, corresponding to a damped harmonic oscillation around 2 GHz. This frequency is represented by the letter B at Figs. 9 and 10, and is related to the SOA relaxation and carrier lifetime. However, the dynamics of SOA switching are complex, and the measured fluctuations after the SOA gain rising have complex shapes and smaller amplitudes.

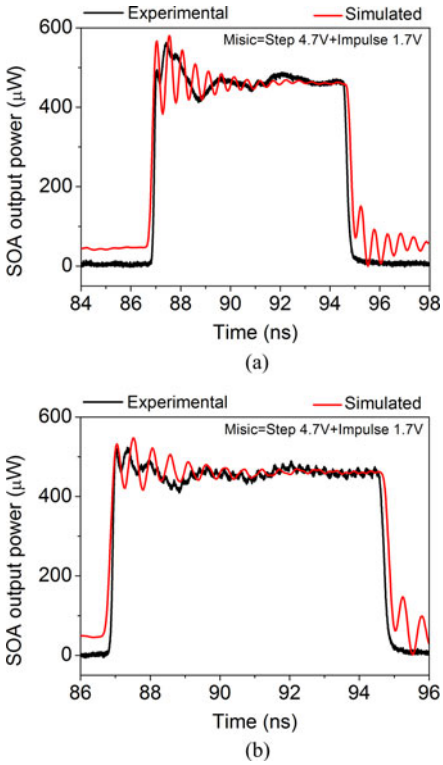

Fig. 12. Experimental and simulated SOA optical response, for impulse = 1.7 V and step of 4.7 V (a) PISIC e (b) MISIC1.

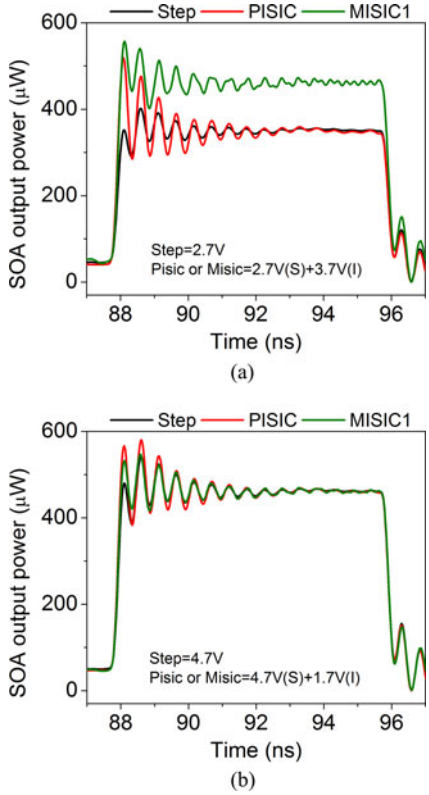

Fig. 13. Simulated SOA optical responses for a single step bias current, PISIC, and Misic1 formats ($I_{\mathrm{DC}} = 80$ mA), for impulse = 3.7 V and step of 2.7 V (a) and impulse = 1.7 V and step of 4.7 V (b).

Therefore, MISIC should act directly on the relaxation oscillations and this is a potential advantage of this technique. Even with these limitations the simulated results predict, and experiments confirm, the smaller fluctuation for the MISIC signals in relation to PISIC format (see Fig. 13). Also, in a first approximation the SOA gain fluctuations can be estimated by simulation.

Other SOAs have been tested and ECs obtained (not shown here). The EC of Fig. 11(b) is valid for other SOAs with few modifications on the parameters values. Therefore, the results presented here should be valid for another SOAs in the sense that MISIC can improve fluctuations due to the relaxation and also provides faster rise times in relation to PISIC.

Based on this fairly good agreement, simulated version of results from Fig. 7 is presented in Fig. 13, demonstrating the same behaviour: reduction of the overshoot by the Misic1 format without worsening the *off-on* switching times. It should be note that EC analysis may be used in SOA-COC manufacturing design in order to relate intrinsic SOA parameters with the switching behaviour, as well as to study the better pulse formats to be applied in electrical-optical switches based on semiconductor gain media.

The experimental results for $I_{\mathrm{DC}} = 60$ mA are shown in Fig. 14, with best performance for Misic6. The Misic5 format had the worst switch time although presents great overshoot reduction. The Misic1 format presents a good performance but not the best as before, showing that the best format is also dependent on the I_{DC}.

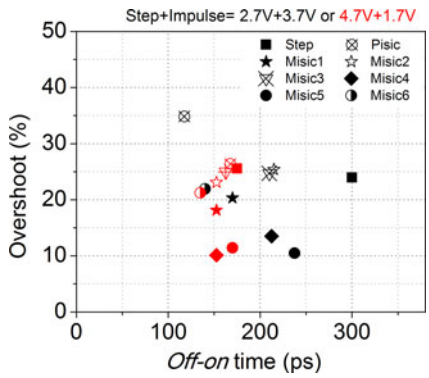

Fig. 14. Overshoots and *off-on* times for different pulse formats ($I_{\mathrm{DC}} = 60$ mA, pre-impulse of 3.7 V and step of 2.7 V or pre-impulse of 1.7 V and step of 4.7 V).

Fig. 15 shows the optical response for the single step, the PISIC and the Misic6 formats, for impulse of 3.7 V and step of 2.7 V (a) and impulse of 1.7 V and step of 4.7 V (b) (for $I_{\mathrm{DC}} = 60$ mA). The increase in optical contrast is clear, with reduction of relative overshoot incidence. The *off-on* time is similar for Misic6 and PISIC formats, much shorter than the obtained for simple step format with 2.7 V (300 ps).

The comparison between pulses with different bias currents shows that the MISIC technique works for all cases, although the best formats has a dependence of how close the total signal is to the gain saturation level. The overshoot reductions

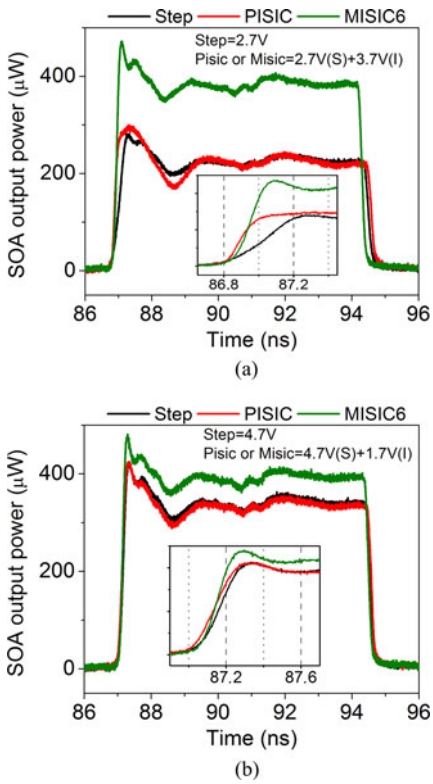

Fig. 15. Optical response for a step injected current, Pisic, and Misic6 formats ($I_{\mathrm{DC}} = 60$ mA), with impulse = 3.7 V for step of 2.7 V (a) and impulse of 1.7 V for step of 4.7 V (b).

enable a relative decrease around 50% (while the *off-on* times are kept constant) in comparison to the simple step and the PISIC formats.

The fluctuations decrease is important to improve the signal reception quality, reducing bit errors. Other advantage of MISIC may be its flexibility since the signal format can be constructed using adequate bit combinations for each desired I_{DC}. The MISIC also could be used in directly modulation of VCSELs, which are used in optical interconnects, increasing the modulation speed of those lasers.

In future applications of recirculating buffers based on SOA-gate arrays [16], [17], a multi-level, phase-modulated optical carrier might be the choice and the SOA chirp during switching would be relevant. The SOA chirp would affect even amplitude-modulated signals when passing further by optical filters, inducing so frequency-to-amplitude conversion. It is interesting to note that the laser chirp is mostly relevant during the SOA gain rising, in the *off-on* electro-optical switching [18]. Therefore, the faster rise times obtained with the MISIC technique would present a smaller time interval of chirp occurrence.

It should be noted that during the *on-off* switching the SOA suffers a carrier depletion. Experimental results [10] shows that PISIC can decrease the *on-off* time by depleting the SOA faster than a single step down. However, the MISIC technique would not be necessary in this case since there is no gain fluctuation after the *on-off* time interval.

A linear SOA must be provided in applications such as optical space switches to avoid inter-channel cross-talk. Those high-linear devices, with bigger active volume, generally would need higher bias currents, and the electro-optical switching would require a stronger microwave signal. Since very fast broadband microwave amplifiers hardly surpass 9 V peak the ac current excursion would be just 150 mA, not enough to provoke deep gain saturation for PISIC and MISIC techniques. However, the conclusions presented here about MISIC advantages and EC models can be applied for linear devices, as soon as SOA gain excursion from below transparency to deeply saturation is obtained using an electrical signal with a rise time (10–90%) faster than 50 ps.

V. Conclusion

Experimental results of electro-optical switching based on SOA-COC were presented. *Off-on* times of 175 ps with optical contrast of 33 dB were obtained by simple-step current in a nonlinear device, which tends to present fast switching times. Besides, the 2-mm-long active region and the high bias current can provide better input power dynamic range, enabling faster operation [19]. By using the PISIC format the switching times are reduced to 115 ps but with high overshoots and fluctuations, issues minimized using MISIC formats. MISIC provides fast switching times due the first, stronger impulse added to the single step, as for the PISIC format, but its further sequence of short pulses counteracts the output power fluctuations inherent to the gain relaxation, and at the same time increases the average injected current, improving the desired optical contrast.

MISIC is demonstrated as an efficiency technique to reduce the residual fluctuations in the SOA output: *off-on* times of 115 ps with small overshoot and high optical contrast were achieved for a SOA-COC. This reduction in switching time is important to decrease the guard band in the switching window. The numerical results based on equivalent-circuit modelling may contribute to the design of faster SOA-based devices, and to the study of different pulse formats promoting improvement of EO switching speeds. Future implementations of SOA-based electro-optical switches should use integrated components, including the microwave (RF) and optical parts.

References

[1] C. Kachris and I. Tomkos, "A Survey on optical interconnects for data centers," *IEEE Commun. Surv. Tutorials*, vol. 14, no. 4, pp. 1021–1036, Apr. 2012.

[2] S. Di Lucente, J. Luo, R. Pueyo Centelles, A. Rohit, S. Zou, K. A. Williams, H. J. S. Dorren, and N. Calabretta, "Numerical and experimental study of a high port-density WDM optical packet switch architecture for data centers," *Opt. Exp.*, vol. 21, no. 1, pp. 263–269, Jan. 2013.

[3] A. Shacham and K. Bergman, "An experimental validation of a wavelength-striped, packet switched, optical interconnection network," *IEEE J. Lightw. Technol.*, vol. 27, no. 7, pp. 841–850, Apr. 2009.

[4] D. Brunina, D. Liu, and K. Bergman, "An energy-efficient optically connected memory module for hibrid packet- and circuit-switched optical networks," *IEEE J. Sel. Topics Quantum Electron.*, vol. 19, no. 2, p. 3700407, Mar./Apr. 2013.

[5] W. Miao, J. Luo, S. Di Lucente, H. Dorren, and N. Calabretta, "Novel flat datacenter network architecture based on scalable and flow-controlled optical switch system," *Opt. Exp.*, vol. 22, no. 3, pp. 2465–2472, Feb. 2014.

[6] H. Wang, E. T. Aw, K. A. Williams, A. Wonfar, R. V. Penty, and I. H. White, "Lossless multistage SOA switch fabric using high capacity monolithic

4×4 SOA circuits," presented at the Opt. Fiber Commun. Conf., OSA, San Diego, CA, USA, Paper S.OWQ2, 2009.
[7] C. M. Gallep and E. Conforti, "Reduction of semiconductor optical amplifier switching times by pre-impulse-step injected current technique," *IEEE Photon. Technol. Lett.*, vol. 14, no. 7, pp. 902–904, 2002.
[8] M. Ikeda, "Switching characteristics of laser diode switch," *IEEE J. Quantum Electron.*, vol. 19, no. 2, pp. 157–164, Feb. 1983.
[9] E. Conforti and C. M. Gallep, "A fast electro-optical amplified switch using a resistive combiner for multi-pulse injection," in *Proc. IEEE MTT-S Int. Microw. Symp. Dig.*, 2006, pp. 1935–1938.
[10] N. S. Ribeiro, A. L. Toazza, C. M. Gallep, and E. Conforti, "Rise time and gain fluctuations of an electrooptical amplified switch based on multipulse injection in semiconductor optical amplifiers," *IEEE Photon. Technol. Lett.*, vol. 21, no. 12, pp. 769–771, May 2009.
[11] V. Francois and F. Lamaree, "Multicore fiber optimization for application to chip-to-chip optical interconnects," *IEEE J. Lightw. Technol.*, vol. 31, no. 24, pp. 4022–4028, Dec. 2013.
[12] R. C. Figueiredo, E. C. Magalhaes, N. S. Ribeiro, C. M. Gallep, and E. Conforti, "Equivalent circuit of a semiconductor optical amplifier chip with bias current influence," in *Proc. IEEE Microw. Optoelectron. Conf.*, 2011, pp. 852–856.
[13] H. Ghafouri-Shiraz, *Fundamentals of Laser Diode Amplifiers.* New York, NY, USA: Wiley, 1996.
[14] R. S. Tucker, "Large-signal circuit model for simulation of injection laser modulation dynamics," in *Proc. Inst. Electr. Eng.*, vol. 128, pt. I, pp. 180–184, 1981.
[15] R. S. Tucker and D. J. Pope, "Circuit modeling of the effect of diffusion on damping in a narrow-stripe semiconductor laser," *IEEE J. Electron.*, vol. QE-19, pp. 1179–1183, Jul. 1983.
[16] E. F. Burmeister, D. J. Blumenthal, and J. E. Bowers, "A comparison of optical buffering technologies," *Opt. Switching Netw.*, vol. 5, no. 1, pp. 10–18, 2008.
[17] E. F. Burmeister, J. P. Mack, H. N. Poulsen, J. Klamkin, L.A. Coldren, D. J. Blumenthal, and J. E. Bowers, "SOA gate array recirculating buffer with fiber delay loop," *Opt. Exp.*, vol. 16, no. 12, pp. 8451–8456, 2008.
[18] M. Matsuura, N. Iwatsu, K. Kitamura, and N. Kishi, "Time-resolved chirp properties of SOAs measured with an optical bandpass filter," *IEEE J. Lightw. Technol.*, vol. 20, no. 23, pp. 2001–2004, Dec. 2008.
[19] R. Bonk, T. Vallaitis, J. Guetlein, C. Meuer, H. Schmeckebier, D. Bimberg, C. Koos, W. Freude, and J. Leuthold, "The input power dynamic range of a semiconductor optical amplifier and its relevance for access network applications," *IEEE Photon. J.*, vol. 3, no. 6, pp. 1039–1053, Dec. 2011.

Rafael C. Figueiredo was born in Vinhedo-SP, Brazil, in 1982. He received the Technologist degree in telecommunications and the M.Sc. degree in electrical engineering from University of Campinas, Campinas-SP, Brazil, in 2007, and 2010, respectively. He is currently working toward the Ph.D. degree at the Optical Communications and Microwave Research Laboratory. His current research interests include semiconductor optical amplifiers, all-optical switching, high-speed all-optical signal processing, and embedded systems.

Napoleão S. Ribeiro received the B.Sc. degree in telecommunications engineering from the Military Engineering Institute, Brazil, in 2003, the M.Sc. and the Ph.D. degrees in electrical engineering from University of Campinas, Campinas, Brazil, in 2006 and 2009, respectively, where he has been a Postdoctoral Researcher, since 2010. His research interests include all optical switching, high-speed all-optical signal processing, and passive optical networks.

Antonio Marcelo Oliveira Ribeiro was born in Brazil in 1970. He received the B.S., M.Sc., and Ph.D. degrees from the School of Electrical and Computer Engineering, University of Campinas, Campinas, Brazil, in 2001, 2004, and 2013, respectively. His research interests include microwave radio propagation and pulse generation, wireless communication systems, short-term statistical channels models, channel characterization, and optical pulse generation.

Cristiano M. Gallep received the B.Sc., M.Sc., and Ph.D. degrees in electrical engineering from the University of Campinas (UNICAMP)/BR, Campinas, Brazil, in 1997, 1999, and 2003, respectively. He is currently an Assistant Professor at UNICAMP, coordinating the Applied Photonics Lab. (LaFA, FT) and collaborating with LAPCOM (FEEC) in applied photonics research—-biophotonics and all-optical signal processing in fiber networks.

Evandro Conforti (S'81–M'83–SM'92–LSM'15) was born in S. J. Rio Preto, SP, Brazil, on August 30, 1947. He received the B.Sc. degree in electronic engineering from the Technological Institute of Aeronautics, Brazil, in 1970, the M.Eng. degree from Federal University of Paraiba, Paraiba, Brazil, in 1972, the M.A.Sc. degree from University of Toronto, ON, Canada, in 1978, and the Ph.D. degree in electrical engineering from State University of Campinas (Unicamp), Brazil, in 1983. He has been with Unicamp since 1981, where he was the Dean of the Faculty of Electrical and Computer Engineering (FEEC) (1984–1987) and is currently a Invited Professor of electrical engineering at FEEC. He was a Visitor at the University of Illinois at Urbana-Champaign (1992–1994) working with the research team of Prof. S.-M. (Steve) Kang. He holds 14 patents and is the coauthor of a book and more than 170 papers in Brazilian and international journals and conferences. He has graduated 10 Ph.D. students and 28 M.Sc. students. His current research interests include semiconductor optical amplifiers, optical coherent communication, all optical switching and electromagnetic measurements. He received the "Academic Merit Medal Prof. A. J. Giarola," Brazilian Society of Microwaves and Optoelectronic (SBMO) 2014; "Unicamp Inventors Prize" 2013; "1° Werner von Siemens Technologic Innovation Prize" (3° place Cat. Researcher), Siemens Brazil 2005; the "Zeferino Vaz Academic Achievements Prize," Unicamp 2005; the "1998 Brazilian Invention Prize"; and the "1983 Unicamp Research Prize."